

Article

Synthesis of Copper Nanoparticles Supported over Graphene-like Material Composite as a Catalyst for Hydrogen Evolution

Qui Quach^{1,2}, Erik Biehler^{1,2}  and Tarek M. Abdel-Fattah^{1,2,*} ¹ Applied Research Center at Thomas Jefferson National Accelerator Facility, Newport News, VA 23606, USA² Department of Molecular Biology and Chemistry, Christopher Newport University, Newport News, VA 23606, USA; qui.quach.13@cnu.edu (Q.Q.); erik.biehler.16@cnu.edu (E.B.)

* Correspondence: fattah@cnu.edu

Abstract: The need for an alternative energy source that is both clean and abundant has led to research into a hydrogen economy. Hydrogen gas can be produced slowly via the hydrolysis of sodium borohydride (NaBH₄). A catalyst can be used to speed up the rate at which hydrogen is produced, however many catalysts involve relatively expensive materials like precious metals. This study explores a novel copper nanoparticle supported on a graphene-like material composite as a catalyst for the hydrolysis of NaBH₄. The material was characterized via powdered X-ray diffraction (P-XRD), Fourier transform infrared spectroscopy (FTIR), transmission electron microscope (TEM), and Energy Dispersive spectroscopy (EDS). The P-XRD confirmed the crystallinity structures of graphene-like material (GLM) and copper nanoparticles supported over graphene-like material (CuGLM). The P-XRD spectra indicated the (110), (111), and (200) lattice planes of copper nanoparticles. In FTIR analysis, the shifted and sharpening functional group peaks were observed when copper nanoparticles were supported by the GLM template. The TEM result indicated that the copper nanoparticle had a size of approximately 10 nm. The catalyst (CuGLM) was tested under different doses of NaBH₄, solution pH, and reaction temperatures. Temperature data were used to determine the activation energy of the reaction to be 46.8 kJ mol⁻¹, which is competitive when compared to similar catalysts. The catalyzed reaction generated the highest volume of hydrogen at pH 8 (51 mL), 303 K (32 mL), and 1225 μmol of NaBH₄ (37 mL). The catalyst was found to be able to be used multiple times in succession without any significant loss in hydrogen generated. This catalyst is an exciting option for the sustainable generation of hydrogen gas as a fuel source.

Keywords: hydrogen; catalysis; energy; nanomaterials; carbon; copper; sustainability; metals

Citation: Quach, Q.; Biehler, E.; Abdel-Fattah, T.M. Synthesis of Copper Nanoparticles Supported over Graphene-like Material Composite as a Catalyst for Hydrogen Evolution. *J. Compos. Sci.* **2023**, *7*, 279. <https://doi.org/10.3390/jcs7070279>

Academic Editor: Francesco Tornabene

Received: 29 May 2023

Revised: 28 June 2023

Accepted: 28 June 2023

Published: 6 July 2023



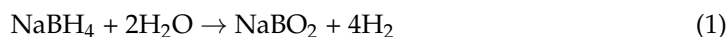
Copyright: © 2023 by the authors. Licensee MDPI, Basel, Switzerland. This article is an open access article distributed under the terms and conditions of the Creative Commons Attribution (CC BY) license (<https://creativecommons.org/licenses/by/4.0/>).

1. Introduction

The combustion of fossil fuel resources to power the world is currently one of the largest contributors to anthropogenic greenhouse gas emissions [1]. It had been observed that the pollution emission of fine particles with diameter of 2.2 μm (PM_{2.5}) can be linked to the premature mortality of people on a global scale [2]. A study by Lelieveld et al. estimated that the removal of fossil fuels is not only beneficial to human health but would also solve the increasing global temperature and issues with the hydrologic cycle [3]. Thus, many studies have been conducted to search for environmentally friendly energy sources which are capable of replacing fossil fuels [4–6]. Among the potential energy sources, hydrogen appears as an ideal candidate due to its abundance, high specific energy, and clean byproduct when combusted as fuel [7,8]. There are some barriers which prevent the widespread application of hydrogen in the energy system. Even though the hydrogen fuel cell is believed to be an effective technology for promoting hydrogen-based energy, there are still some challenges that lie in hydrogen production and storage [9,10]. Currently, hydrogen is primarily produced from fossil fuel resources such as natural gas, methane,

and coal [11,12]. In order for hydrogen to contribute a significant role in low-carbon future and a secure energy system, it would be essential to reduce the fossil dependence [13,14]. Since hydrogen has a low density, a specific type of storage tank is required for transporting the fuel. Compared to gasoline, hydrogen requires a higher volume to store; however, hydrogen possesses a higher energy yield than gasoline [15,16]. The storage of hydrogen has met various challenges. The most common methods for storing hydrogen are through high-pressure gas cylinders or in cryogenic tanks; however, these methods require a delicate control of pressure and temperature [17]. A liquid nitrogen tank is required to have a double wall structure as a thermal insulation to keep a low temperature condition [18]. Regarding the high-pressure tanks of a natural gas vehicle, it is estimated to require 20–25 MPa to compress the gas [18]. Additionally, when the pressure is doubled, the amount of hydrogen stored is only increased up to 40–50% [18]. In order to tolerate the high pressure, the tank must be made from carbon composite V3 and V4 [18].

An alternative method of hydrogen storage avoids the problems associated with pressure and temperature by storing it within the structure of borohydride compounds [19]. Metal borohydrides are found to be thermostable hydrogen storage materials which can reversibly store hydrogen at high density, with only moderate temperature and pressure [20]. For example, LiBH_4 in solid form only releases a small amount of hydrogen when the temperature increases between 100 °C and 200 °C [19]. The solid form of sodium borohydride starts to release hydrogen when heated up to 470 °C [19]. Among the metal borohydrides, sodium borohydride (NaBH_4) appears to be the optimal compound for a hydrogen evolution reaction as it contains roughly 10.8% hydrogen by weight [21]. Additionally, this compound is able to release hydrogen gas in the presence of water as displayed in Equation (1):



The application of NaBH_4 in generating hydrogen still faces challenges in optimizing the reaction rate. Many studies on catalysts have been conducted to enhance the hydrogen evolution of this reaction [22–26]. Among the catalysts, nanoparticles have shown their potential in enhancing the hydrogen generation reaction rates, and different factors like nanoparticle size and use of a support template contribute to the catalytic capability of nanoparticles [23–30]. Well-dispersed nanoparticles improve their surface area and catalytic ability; however, nanoparticles have a tendency to agglomerate [28–30]. The agglomeration of nanoparticles may also lead to strain effects and lattice defects which impact the catalytic property of nanoparticles [29]. It has been shown that the use of a support template can increase the available surface area of nanomaterials [30,31] and assists in preventing the agglomeration while also improving the catalytic performance of nanoparticles [32,33].

Previous studies have shown that precious metal nanoparticles such as gold, silver, and platinum are effective in tuning optoelectronic properties [34], antibacterial uses [35], and enhancing the rate of hydrogen generation reactions [36,37]. While these precious metals are good choices as catalysts, they are often expensive. Many cheaper metals such as nickel and copper have been studied and shown to be as catalytically effective as the precious metals [38,39]. Copper-based catalysts have been extensively researched and found to be efficient in supporting the hydrogen fuel cell [40,41]. In the study of Wu et al. (2004), when copper nanoparticles are incorporated into TiO_2 system, the hydrogen evolution reaction (HER) catalytic activity was increased by 10 times [42].

Graphene-like materials (GLMs) were chosen as a carbon support template for enhancing the dispersing of copper nanoparticles. After the invention of graphene, scientists have been focusing on investigating 2D materials with similar structure and properties to that of graphene [43,44]. Although graphene appears to be an excellent support framework for different nanoparticles, the production of graphene often requires toxic chemicals and has an elevated risk of combustion [45,46]. There are many GLMs that can be synthesized from cheap biomass such as glucose and plant-based materials and can be as effective as graphene in dispersing the nanoparticles [47,48]. Previous studies have shown that copper

nanoparticles are highly compatible with 2D graphene structures and have been used to support the growth of graphene [49,50].

In our study, copper nanoparticles embedded on graphene-like materials (CuGLM) was synthesized and structurally characterized by Powder X-ray Diffraction (P-XRD), Scanning Electron Microscopy coupled with Energy Dispersive X-ray Spectroscopy (SEM-EDS), Fourier transform infrared spectroscopy (FTIR), and Transmission Electron Microscopy (TEM). Various conditions such as pH, temperature, NaBH_4 dosage, and reusability were considered in examining the catalyzed effect of CuGLM on hydrogen evolution reaction.

2. Experimental

2.1. Synthesis of Graphene-like Material

The method of Adel et.al. was applied and slightly modified to synthesize graphene-like material [47]. A volume of 20 mL of 0.5 M of dextrose solution was added to 50 mL Teflon-lined autoclave tubes. The solution was autoclaved at 200 °C for 4 h, and then cooled to room temperature. The product was collected by being centrifuged at 15,000 rpm for 30 min, and then washed with DI water several times. After that, the brown precipitates were dried in the oven at 100 °C overnight.

2.2. Synthesis of Copper Nanoparticle and CuGLM

The method of Xiong et.al. was applied to synthesize copper nanoparticles [51]. A volume of 50 mL of 0.2 M $\text{CuCl}_2 \cdot 2\text{H}_2\text{O}$ aqueous solution was prepared in a flask and heated to 80 °C while stirring. After that, 50 mL of 0.8 M L-ascorbic acid aqueous solution was added dropwise to the flask. The mixture was stirred and kept at 80 °C until a dark red solution was formed. The solution was cooled to room temperature and then centrifuged at 8000 rpm for 15 min to remove unreacted reactants.

The incipient wetness method was applied to connect the nanoparticles to the GLM structure. A few milliliters of nanoparticles solution were added to the GLM and then dried in the oven at 50 °C. The process was repeated several times.

2.3. Characterization

The crystal structures of CuNPs and GLMs were identified through powder X-ray diffraction (P-XRD, Rigaku Miniflex II, Cu $K\alpha$ X-ray, nickel filters). Each sample was spread flat on sample holding plate and scanned from 5° to 90°.

Fourier transform infrared spectroscopy (FTIR, Shimadzu IR-Tracer 100, Kyoto, Japan) with an Attenuated Total Reflectance (ATR, Shimadzu QATR-S, Kyoto, Japan) attachment was used to confirm the functional group of the nanocomposite. The presence of Cu nanoparticles on GLM was confirmed by Scanning Electron Microscopy (SEM, JEOL JSM-6060LV, Akishima, Tokyo) and energy dispersive X-ray spectroscopy (EDS, ThermoScientific UltraDry, Waltham, MA, USA).

For transmission electron microscopy (TEM, JEM-2100F) characterization, a few drops of copper nanoparticles were added to the carbon grid. Regarding the CuGLM, the nanocomposite powder was mixed with 3 mL of DI water and sonicated for 10 min. A few drops of the solution were added to the copper grid. Both grids were dried in the oven.

2.4. Catalysis

The volume of generated hydrogen was measured by using the gravimetric water displacement system [37,38]. The closed system contained two Buchner flasks. In one flask, 100 mL of DI water was mixed with 0.1 g of CuGLM. NaBH_4 was then added, and generated hydrogen flowed to the other flask that contained 100 mL DI water. Pressure from the hydrogen forced water from the second flask through tubing where it dripped into a cup on a mass balance (Pioneer, OHAUS, Parsippany, NJ, USA). The water displaced over the period of two hours was monitored via the data logging software (SPDC Data Collector, OHAUS, Parsippany, NJ, USA). The pH of the solution was altered (pH 6, pH7,

and pH 8) by using nitric acid or sodium hydroxide. Temperature conditions (283 K, 288 K, 295 K, 303 K) of the reactions were controlled by using a water bath system. The reaction was also examined under various doses of NaBH_4 (625 μmol , 925 μmol , 1225 μmol). Lastly, reusability trials occurred using conditions at pH 7 and at 295 K. A 925 μmol NaBH_4 dosage was supplied for a two-hour trial. Immediately after two hours, a second 925 μmol dose was added, marking the start of a second trial. This was repeated for a total of five trials.

3. Results

Images of the novel CuGLM catalyst were taken using TEM. Figure 1A depicts clumped masses of GLM support material. Figure 1B shows the multilayers of the graphene-like material. Small nanoparticles can be seen in Figure 1B,C, allowing for an average nanoparticle size of 13 nm to be determined.

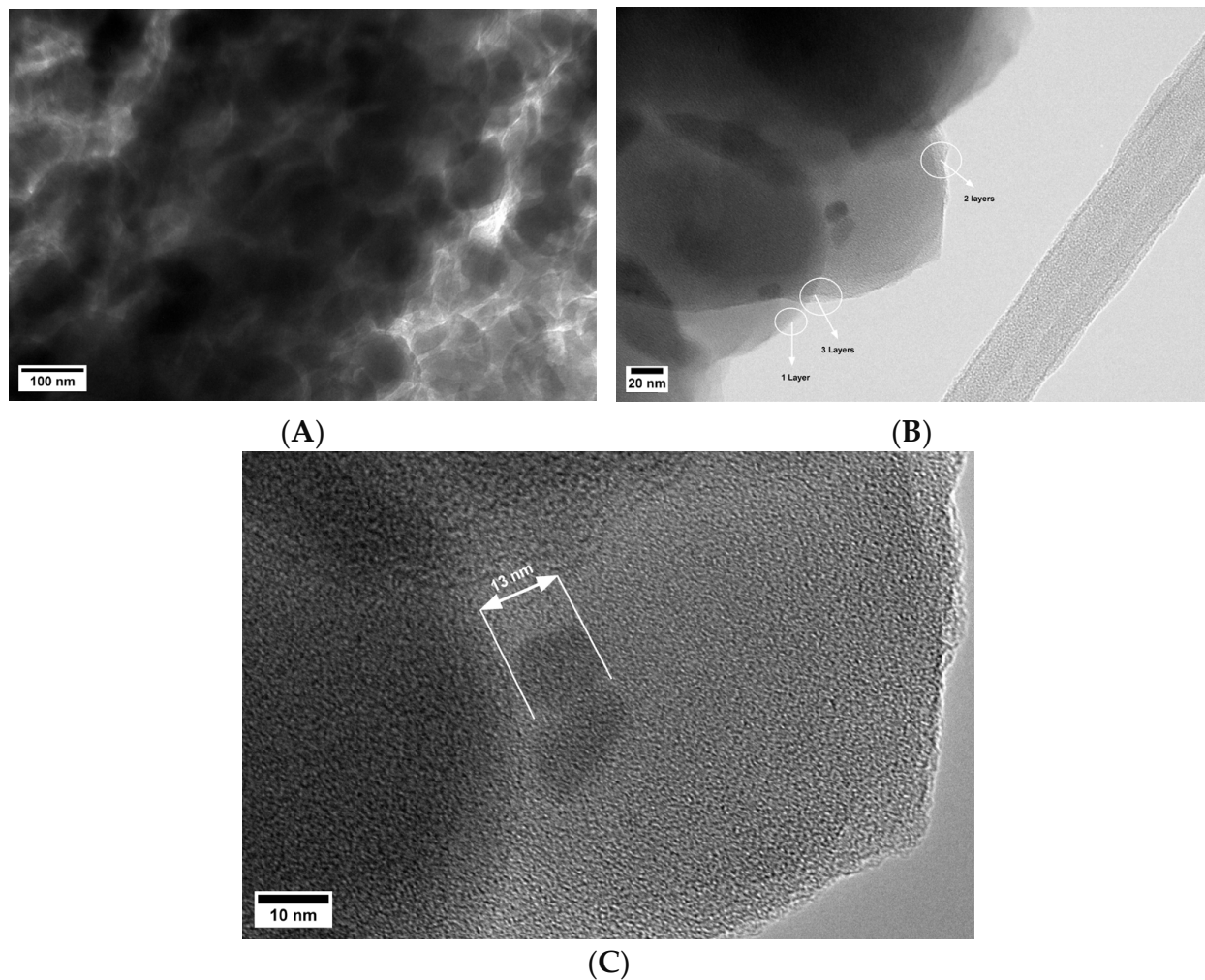


Figure 1. TEM images of the CuGLM composite material at scales of 100 nm (A), 20 nm (B), and 10 nm (C).

CuGLM catalyst was characterized via the EDS analysis from SEM images (Figure 2). The spectra shows that the elements in the sample in the order of most abundant to least were carbon, oxygen, and then copper. Despite the small weight percentage of 0.56%, this analysis confirmed the presence of copper within the sample which can be attributed to the nanoparticles seen in Figure 1.

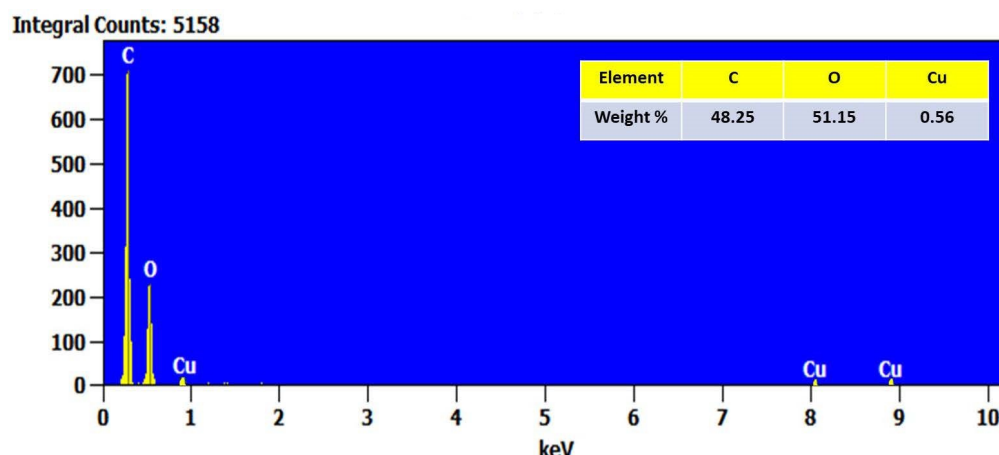


Figure 2. EDS spectrum of the CuGLM catalyst and elements weight%.

XRD analysis was used to further characterize the CuGLM composite and was compared to GLM with no nanoparticles (Figure 3). The GLM showed only one large broad peak around 22° which can be attributed to the graphitic characteristics of the carbon-based backbone material [52]. The CuGLM also experienced this peak as much of the material was the GLM support. A very sharp peak was seen at both 28.7° and 33.2° which can be associated with the (110) and (111) lattice plane of copper oxide, respectively (JCPDS 48-1548) [53,54]. Two peaks of copper nanoparticles can be seen at 47.6° and 56.4° which are indicative of the (111) and (200) faces, respectively, despite being shifted up roughly 5° each [55]. This shifting has been reported before as nanoparticles can change the lattice structure of carbon-based materials [56].

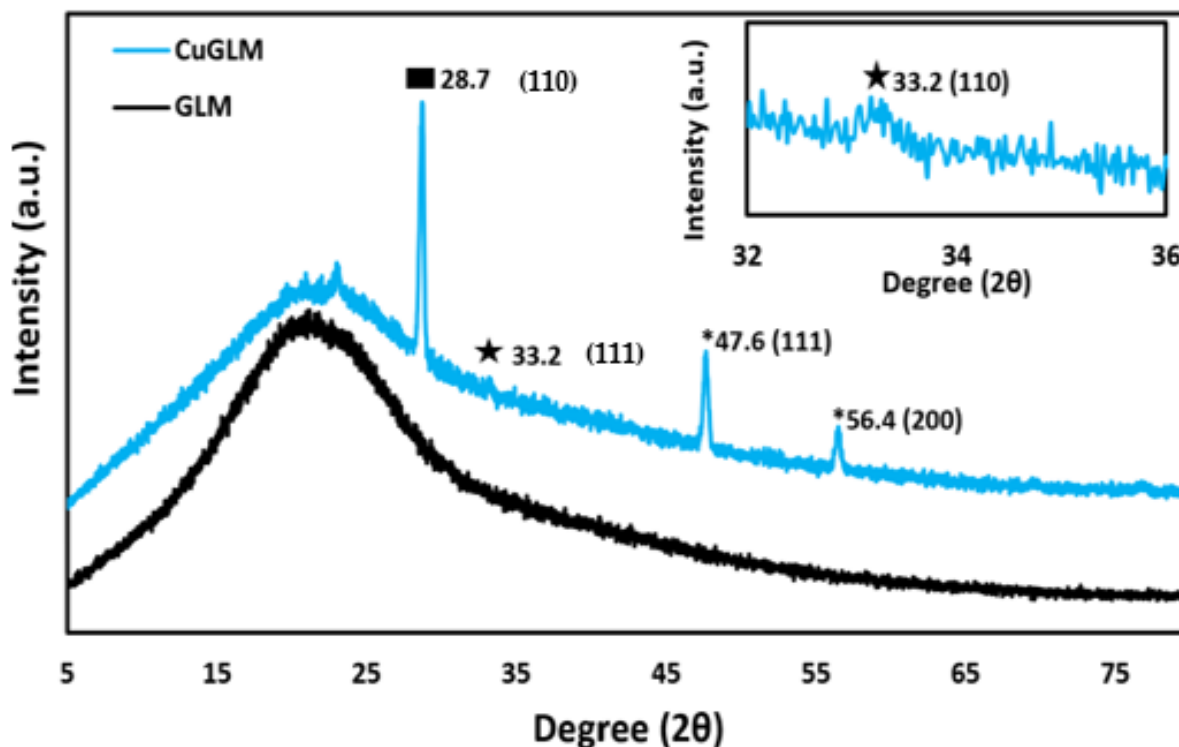


Figure 3. XRD analysis of CuGLM and GLM. Rectangles represent peaks associated with copper chloride, stars represent copper oxide peaks, and asterisks represent the peaks of copper nanoparticles. The inset graph highlights the peak at 33.2°.

FTIR analysis was performed on CuGLM to detect the presence of functional groups (Figure 4). The unsupported GLM shows a broad peak ranging from roughly 3600 cm^{-1} to 3000 cm^{-1} and is indicative of an OH stretch. A short peak at 2900 cm^{-1} is indicative of a C–C bond. A peak at 1700 cm^{-1} indicates the presence of a C=O bond. All three of these peaks are commonly associated with graphitic characteristics and can be attributed to the GLM backbone. The CuGLM composite showed the same set of peaks. When CuNPs are incorporated into the GLM, the C=O and C–C peaks were slightly shifted and had a slightly higher intensity. This indicates that the addition of the copper nanoparticles did not significantly alter the structure of the GLM.

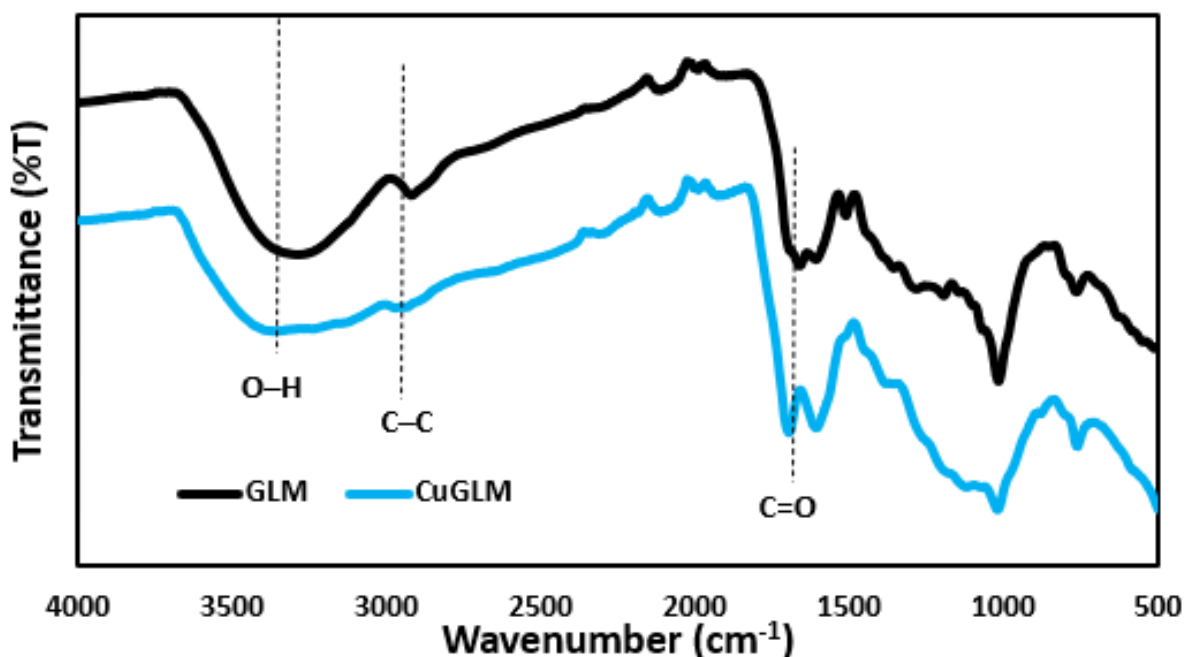


Figure 4. FTIR analysis of CuGLM and unsupported GLM.

With the characterization of the material completed, catalytic trials of CuGLM began, first evaluating the catalyst at NaBH_4 doses of $625\text{ }\mu\text{mol}$, $925\text{ }\mu\text{mol}$, and $1225\text{ }\mu\text{mol}$ (Figure 5). At a dose of $625\text{ }\mu\text{mol}$, the reaction as catalyzed by CuGLM produced roughly 19.0 mL of hydrogen at a rate of $0.0158\text{ mL min}^{-1}\text{ mg}_{\text{cat}}^{-1}$. At an increased NaBH_4 dose of $925\text{ }\mu\text{mol}$, the rate of hydrogen generation increased to $0.0236\text{ mL min}^{-1}\text{ mg}_{\text{cat}}^{-1}$, producing a volume of 27.6 mL after two hours. When the dose of NaBH_4 was further increased to $1225\text{ }\mu\text{mol}$, the volume of hydrogen generated increased even more to 37.6 mL at a rate of $0.0313\text{ mL min}^{-1}\text{ mg}_{\text{cat}}^{-1}$. Based on this data, it is evident that there is a positive linear relationship between the NaBH_4 dosage, and the volume of hydrogen gas produced. This follows Le Chatelier's principle which states an increase in one of the reactants will result in an increase in the products.

The next catalytic study performed for the CuGLM catalyst was at conditions of pH 6, pH 7, and pH 8 (Figure 6). The pH of the reaction was lowered to pH 6 which resulted in a hydrogen generation rate of $0.0430\text{ mL min}^{-1}\text{ mg}_{\text{cat}}^{-1}$ and a volume of 51.6 mL . At pH 7, the reaction generated $0.0236\text{ mL min}^{-1}\text{ mg}_{\text{cat}}^{-1}$, which produced a volume of 27.6 mL . Lastly, when the pH of the solution was raised to 8, the reaction produced 14.7 mL with a generation rate of $0.0125\text{ mL min}^{-1}\text{ mg}_{\text{cat}}^{-1}$. From the above data, it is clear that the reaction proceeds better in acidic conditions. This was explained by the team of Schlesinger et al. who theorized that the extra hydrogen ions in acidic solutions cause the reaction to proceed faster [57]. The observed decrease in hydrogen produced in alkaline conditions is possibly due to an increase in the concentration of metaborate ions in the solution, as noted by Kaufman et al. [58].

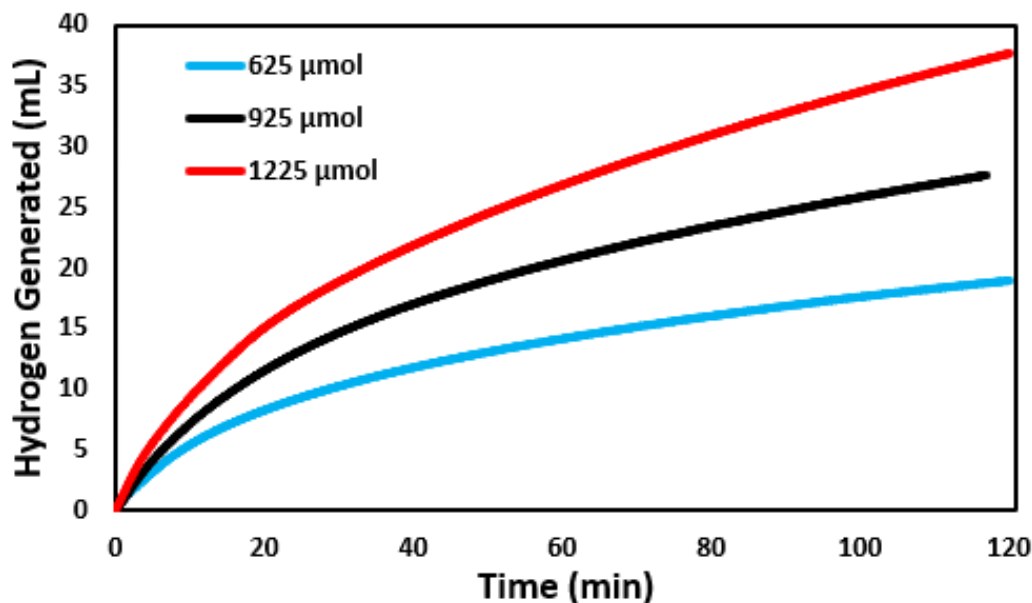


Figure 5. Effect of NaBH_4 dosage on the catalytic ability of CuGLM in 100 mL of DI water.

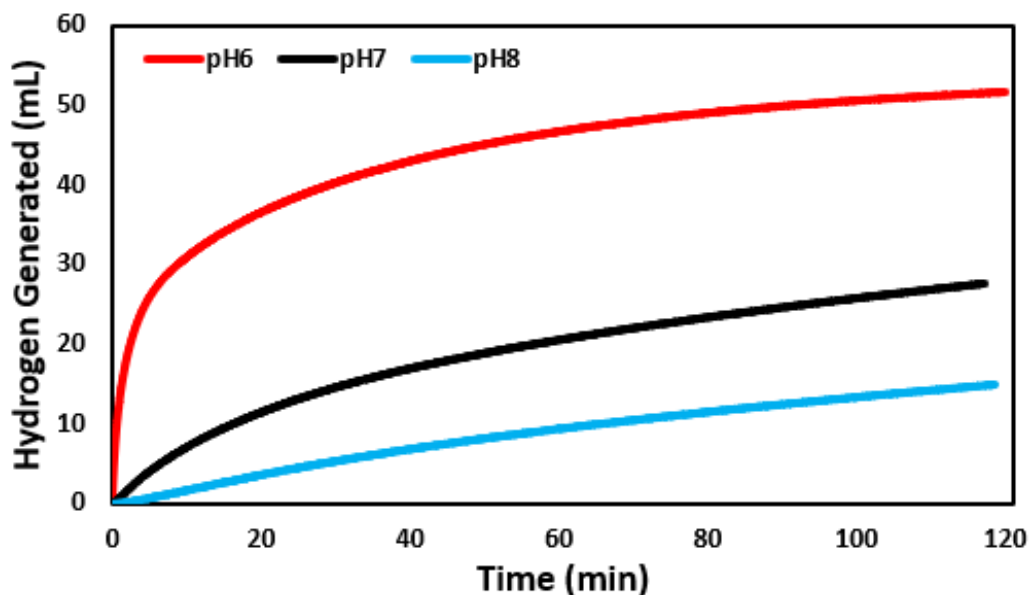


Figure 6. Effect of pH on the catalytic ability of CuGLM.

CuGLM was then evaluated as a catalyst at temperatures of 283 K, 288 K, 295 K, and 303 K (Figure 7). The temperature of the solution was first lowered to 288 K and produced 14.3 mL of hydrogen at a rate of $0.0119 \text{ mL min}^{-1} \text{ mg}_{\text{cat}}^{-1}$. The temperature was then lowered even more to 283 K, which resulted in a decrease in the generation rate to $0.0089 \text{ mL min}^{-1} \text{ mg}_{\text{cat}}^{-1}$ and a volume of 10.6 mL. At room temperature (295 K), the reaction produced 27.6 mL of hydrogen at a rate of $0.0236 \text{ mL min}^{-1} \text{ mg}_{\text{cat}}^{-1}$. Finally, when the temperature of the reaction was raised to 303 K, the volume of hydrogen produced was 32.5 mL at a rate of $0.0271 \text{ mL min}^{-1} \text{ mg}_{\text{cat}}^{-1}$. Figure 7 shows a clear trend that increasing the temperature of the reaction increases the rate at which hydrogen is produced. As with the dosage study, this is in agreement with Le Chatelier's principle.

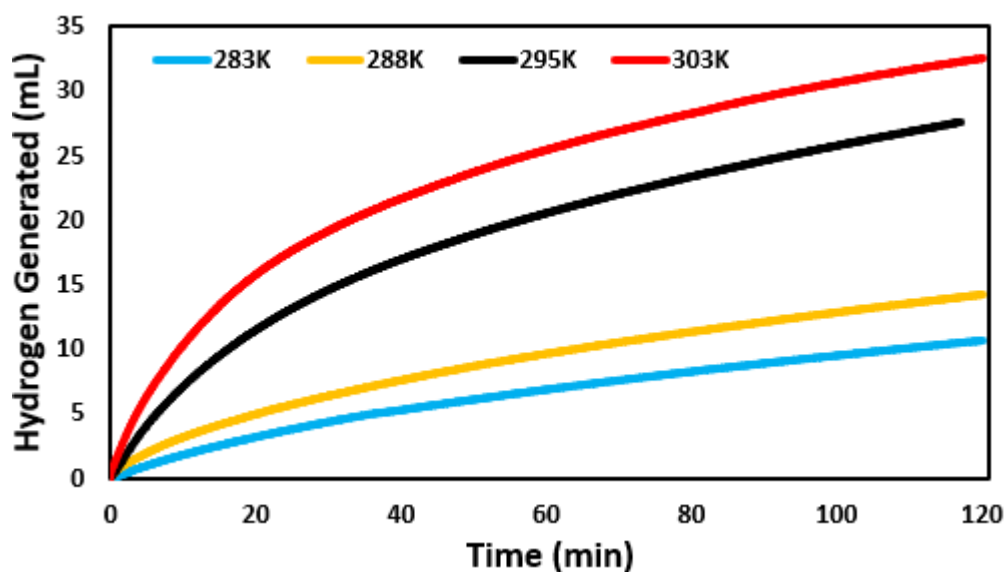


Figure 7. Effect of temperature on the catalytic ability of CuGLM.

From the temperature study, the activation energy of the reaction was able to be found via the Arrhenius Equation (2), where k is the reaction’s rate constant, E_a is the activation energy of the reaction, R is the universal gas constant, T is the temperature of the reaction in kelvin, and A is the preexponential factor.

$$k = Ae^{-\frac{E_a}{RT}} \tag{2}$$

By plugging each temperature tested into Equation (2), the rate constants of the reaction could be determined. The natural log of each rate constant was then plotted against one thousand divided by the coinciding temperature in kelvin to create an Arrhenius plot (Figure 8). The absolute value of the slope of the equation of the line from Figure 8 multiplied by the gas constant allowed the activation energy of the reaction as catalyzed by CuGLM to be determined to be 46.8 kJ mol^{-1} . This activation energy was then compared to similar catalysts for this reaction in Table 1.

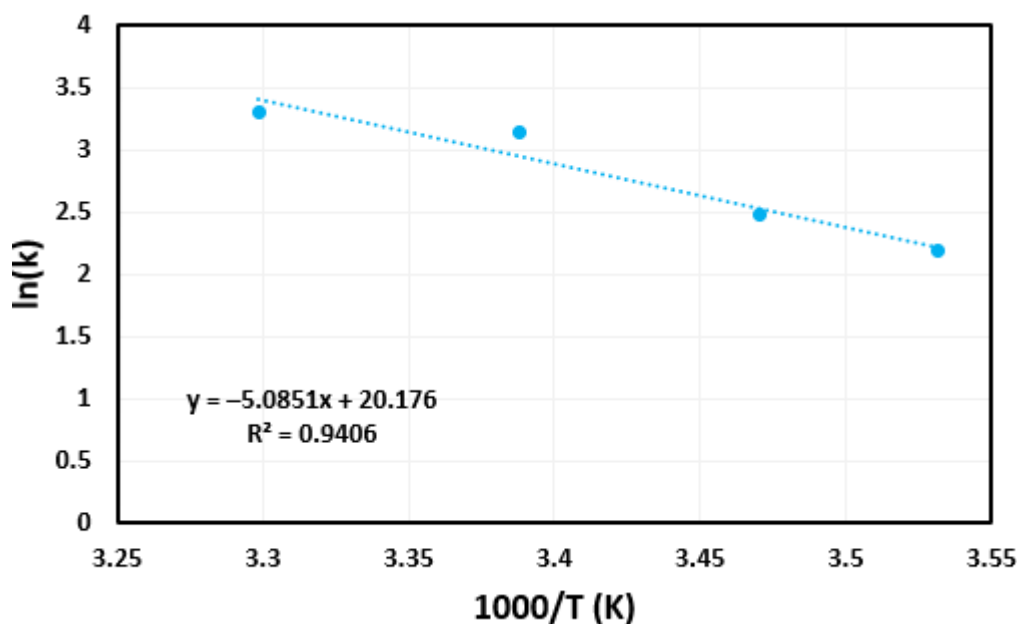


Figure 8. Arrhenius plot created for CuGLM.

Table 1. Table of Reported Activation Energies (E_a kJ mol⁻¹).

Catalyst	E_a (kJ mol ⁻¹)	Temperature (K)	Reference
Ni	71	273–308	[58]
Raney-Nickel	63	273–308	[58]
Co	75	273–308	[58]
Cu based Catalyst	61.2	303	[59]
Co-Cu-B	49.6	293–343	[60]
Pt/MWCNTs	46.2	283–303	[23]
Ag/MWCNTs	44.5	273–303	[61]
Pd/MWCNTs	62.7	273–303	[62]
Au/MWCNTs	21.1	273–303	[63]
BCD-AuNP	54.7	283–303	[36]
Pd Nanocup	58.9	283–303	[64]
PtNPs	39.2	283–303	[65]
CuGLM	46.8	283–303	This Work

Table 1 compares CuGLM to other catalysts for the hydrolysis of NaBH₄. This novel material with its activation energy of 46.8 kJ mol⁻¹ outperforms bulk materials, as well as two other catalysts that contain copper. Most of the other composite catalyst materials explored by this team have an activation energy that is lower than the CuGLM catalyst; however these composites contain precious metals, which are more expensive than copper. The relative inexpensiveness of copper, combined with the simple, sugar-based support and competitive activation energy makes this catalyst a promising choice for this reaction.

For a final test, CuGLM was assessed multiple times for its reusability (Figure 9). Five consecutive trials were run, each lasting two hours and using a dose of 925 μmol of NaBH₄. The reactions were run at pH 7 and 295 K which were ambient lab conditions. Hydrogen production was relatively consistent across the first four trials, despite trial two producing slightly less. The fifth trial produced more than the others, possibly indicating that the catalyst becomes activated with consecutive uses. Overall, the CuGLM catalyst produced an average volume of 27.1 mL across the five trials. The catalyst efficiency increased after consecutive uses could be from the effect of BH₄ and H⁻ formed strong bond on the surface of nanoparticles [66]. Over time, these bonds become hydrolyzed and increase the electrostatic stabilization of the nanoparticle surfaces, which made them more active [66]. This phenomenon had been explained in the study of Deraedt et al. (2014) [66].

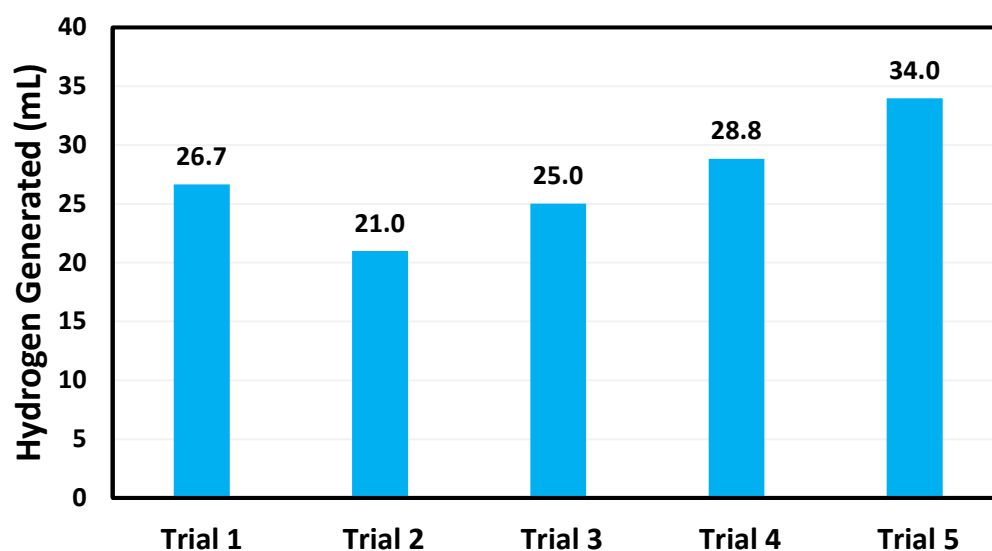
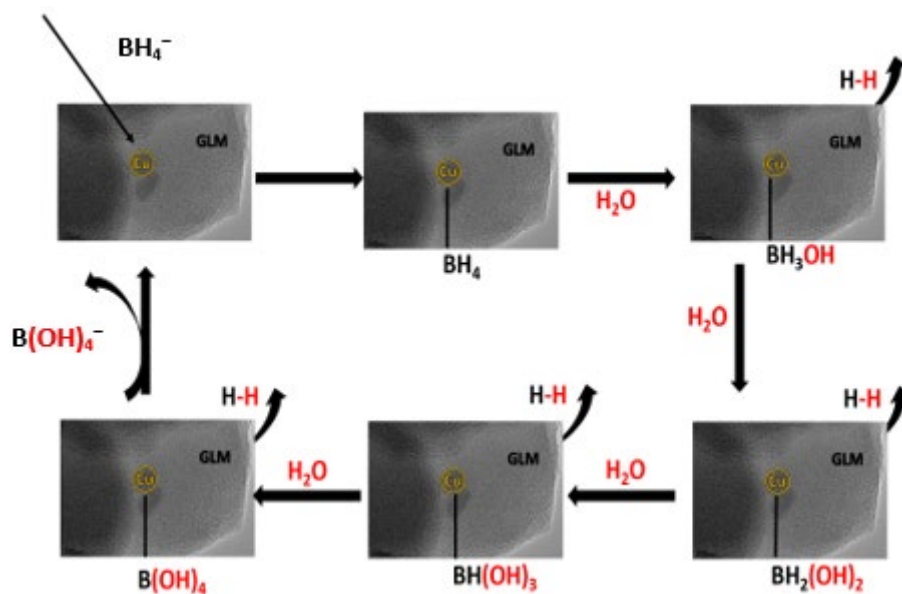


Figure 9. Catalytic reusability of CuGLM. The number on top of each bar is the volume of hydrogen produced by that trial in mL after two hours.

A mechanism by which CuGLM catalyzes the hydrolysis reaction of NaBH_4 is depicted in Scheme 1. In this mechanism, a single borohydride ion (BH_4^-) binds to a single copper nanoparticle. A nearby water molecule then attacks the boron from the BH_4 and replaces one of the hydrogen atoms. As the hydrogen leaves, it bonds to a hydrogen atom from the water molecule, stripping it from the water and forming a gaseous H_2 molecule. This same process will happen for each of the hydrogen atoms on the BH_4 , resulting in four H_2 molecules being released. Once there are no more hydrogen atoms for water to attack, the remaining tetrahydroxyborate [$\text{B}(\text{OH})_4^-$] can unbind from the copper nanoparticle and a new BH_4^- can take its place, repeating the cycle.



Scheme 1. Proposed mechanism by which CuGLM catalyzes the hydrolysis of NaBH_4 .

Finally, the graphene-like materials (GLMs) used in this study showed great promise as catalyst support with agreement with other studies [67–69].

4. Conclusions

We report the successful synthesis of a novel composite catalyst made from copper nanoparticles supported on graphene-like materials. The material was characterized using TEM, EDS, XRD, and FTIR. Catalytic trials were performed under various reaction conditions including dosage of NaBH_4 , pH of solution, and temperature. It was determined that the optimal reaction conditions included larger doses of NaBH_4 , lower pH, and higher temperatures, with the best condition tested being pH 6 which produced hydrogen at a rate of $0.0430 \text{ mL min}^{-1} \text{ mg}_{\text{cat}}^{-1}$. Temperature trials allowed us to determine the activation energy of the catalyst to be 46.8 kJ mol^{-1} , which is competitively low compared to similar catalysts. A reusability study revealed that the catalyst can be used multiple times in a row with a slight decrease in hydrogen produced after the first trial, and then increased amounts with each additional trial. This study indicates that CuGLM is a promising option when choosing a catalyst for the hydrolysis of NaBH_4 . By using a non-precious metal as the catalyst, and sugar as a precursor to the support, this catalyst could be a cheaper option compared to other catalysts. The reusability study indicates that the same amount of material can be utilized multiple times, promoting sustainability.

Author Contributions: E.B.: data curation, formal analysis, writing—original draft. Q.Q.: data curation, formal analysis, writing—original draft. T.M.A.-F.: conceptualization, validation, formal analysis, investigation, resources, supervision, writing—review & editing. All authors have read and agreed to the published version of the manuscript.

Funding: This research received no external funding.

Data Availability Statement: The data presented in this study are available on request from the corresponding author.

Acknowledgments: The Corresponding Author acknowledges the Professorship of Lawrence J. Sacks in Chemistry.

Conflicts of Interest: The authors declare no conflict of interest.

References

1. Hook, M.; Tang, X. Depletion of fossil fuels and anthropogenic climate change-A review. *Energy Policy* **2013**, *52*, 797–809. [[CrossRef](#)]
2. Lelieveld, J.; Evans, J.S.; Fnais, M.; Giannadaki, D.; Pozzer, A. The contribution of outdoor air pollution sources to premature mortality on a global scale. *Nature* **2015**, *525*, 367–371. [[CrossRef](#)] [[PubMed](#)]
3. Lelieveld, J.; Klingmuller, K.; Pozzer, A.; Burnett, R.T.; Haines, A.; Ramanathan, V. Effects of fossil fuel and total anthropogenic emission removal on public health and climate. *PNAS* **2019**, *116*, 7192–7197. [[CrossRef](#)] [[PubMed](#)]
4. Daut, I.; Razliana, A.R.N.; Irwan, Y.M.; Farhana, Z. A Study on the Wind as Renewable Energy in Perlis, Northern Malaysia. *Energy Procedia* **2012**, *18*, 1428–1433. [[CrossRef](#)]
5. Kabir, E.; Kumar, P.; Kumar, S.; Adelodun, A.A.; Kim, K.-K. Solar energy: Potential and future prospects. *Renew. Sustain. Energy Rev.* **2018**, *82*, 894–900. [[CrossRef](#)]
6. Bosnjakovic, M.; Sinaga, N. The Perspective of Large-Scale Production of Algae Biodiesel. *Appl. Sci.* **2020**, *10*, 8181. [[CrossRef](#)]
7. Balat, M.; Balat, M. Political, economic and environmental impacts of biomass-based hydrogen. *Int. J. Hydrog. Energy* **2009**, *34*, 3589–3603. [[CrossRef](#)]
8. Felseghi, R.A.; Carcadea, E.; Raboaca, M.S.; Trufin, C.N.; Filote, C. Hydrogen Fuel Cell Technology for the Sustainable Future of Stationary Applications. *Energies* **2019**, *12*, 4593. [[CrossRef](#)]
9. Staffell, I.; Scamman, D.; Abad, A.V.; Balcombe, P.; Dodds, P.E.; Ekins, P.; Shah, N.; Ward, K.R. The role of hydrogen and fuel cells in the global energy system. *Energy Environ. Sci.* **2019**, *12*, 463–491. [[CrossRef](#)]
10. Garland, N.L.; Papageorgopoulos, D.C.; Stanford, J.M. Hydrogen and fuel cell technology: Progress, challenges, and future directions. *Energy Procedia* **2012**, *28*, 2–11. [[CrossRef](#)]
11. Barbir, F. Transition to renewable energy systems with hydrogen as an energy carrier. *Energy* **2009**, *34*, 308–312. [[CrossRef](#)]
12. Liu, K.; Song, C.; Subramani, V. *Hydrogen and syngas Production and Purification Technologies*; Wiley: Hoboken, NJ, USA, 2009; pp. 1–13.
13. Sheffield, J.W.; Sheffield, C. *Assessment of Hydrogen Energy for Sustainable Development*; Springer: Berlin/Heidelberg, Germany, 2007; pp. 1–8.
14. Dunn, S. Hydrogen futures: Toward a sustainable energy system. *Int. J. Hydrogen Energy* **2002**, *27*, 235–264. [[CrossRef](#)]
15. Kapdan, I.K.; Kargi, F. Bio-hydrogen production from waste materials. *Enzyme Microb.* **2006**, *38*, 569–582. [[CrossRef](#)]
16. Sharma, S.; Ghoshal, S.K. Hydrogen the future transportation fuel: From production to applications. *Renew. Sustain. Energy Rev.* **2015**, *43*, 1151–1158. [[CrossRef](#)]
17. Zuttel, A. Hydrogen storage methods. *Sci. Nat.* **2004**, *91*, 157–172. [[CrossRef](#)]
18. Mori, D.; Hirose, K. Recent challenges of hydrogen storage technologies for fuel cell vehicles. *Int. J. Hydrogen Energy* **2009**, *34*, 4569–4574. [[CrossRef](#)]
19. Puszekiel, J.; Garroni, S.; Milanese, C.; Gennari, F.; Klassen, T.; Dornheim, M.; Pistidda, C. Tetrahydroborates: Development and Potential as Hydrogen Storage Medium. *Inorganics* **2017**, *54*, 74. [[CrossRef](#)]
20. Li, H.W.; Yan, Y.; Orimo, S.I.; Zuttel, A.; Jesen, C.M. Recent progress in metal borohydrides for hydrogen storage. *Energies* **2011**, *4*, 185–214. [[CrossRef](#)]
21. Demirci, U.B. About the Technological Readiness of the H₂ Generation by Hydrolysis of B-(N)-H Compounds. *Energy Technol.* **2018**, *6*, 1–18.
22. Dushatinski, T.; Huff, C.; Abdel-Fattah, T.M. Characterization of electrochemically deposited films from aqueous and ionic liquid cobalt precursors toward hydrogen evolution reactions. *Appl. Surf. Sci.* **2016**, *385*, 282–288. [[CrossRef](#)]
23. Huff, C.; Quach, Q.; Long, J.M.; Abdel-Fattah, T.M. Nanocomposite catalyst derived from ultrafine platinum nanoparticles and carbon Nanotubes for hydrogen generation. *ECS J. Solid State Sci. Technol.* **2020**, *9*, 101008. [[CrossRef](#)]
24. Osborne, J.; Horton, M.R.; Abdel-Fattah, T.M. Gold Nanoparticles Supported Over Low-Cost Supports for Hydrogen Generation from a Hydrogen Feedstock Material. *ECS J. Solid State Sci. Technol.* **2020**, *9*, 071004. [[CrossRef](#)]
25. Huff, C.; Dushatinski, T.; Barzanjii, A.; Abdel-Fattah, N.; Barzanjii, K.; Abdel-Fattah, T.M. Pretreatment of gold nanoparticle multi-walled carbon nanotube composites for catalytic activity toward hydrogen generation reaction. *ECS J. Solid State Sci. Technol.* **2017**, *6*, M69–M71. [[CrossRef](#)]
26. Abdel-Fattah, T.M.; Wixtrom, A. Catalytic Reduction of 4-Nitrophenol Using Gold Nanoparticles Supported On Carbon Nanotubes. *ECS J. Solid State Sci. Technol.* **2014**, *3*, M18–M20. [[CrossRef](#)]
27. Tran, T.D.; Nguyen, M.T.T.; Le, H.V.; Nguyen, D.N.; Truong, Q.D.; Tran, P.D. Gold nanoparticles as an outstanding catalyst for the hydrogen evolution reaction. *Chem. Commun.* **2018**, *54*, 3363–3366. [[CrossRef](#)]
28. Haruta, M. Size- and support-dependency in the catalysis of gold. *Catal. Today* **1997**, *36*, 153–166. [[CrossRef](#)]

29. Jaramillo, T.F.; Baeck, S.H.; Cuenya, B.R.; McFarland, E.W. Catalytic Activity of Supported Au Nanoparticles Deposited from Block Copolymer Micelles. *J. Am. Chem. Soc.* **2003**, *125*, 7148–7149. [[CrossRef](#)]
30. Wu, J.; Li, P.; Pan, Y.T.; Warren, S.; Yin, X.; Yang, H. Surface Lattice-Engineered Bimetallic Nanoparticles and Their Catalytic Properties. *Chem. Soc. Rev.* **2012**, *41*, 8066–8074. [[CrossRef](#)]
31. Biehler, E.; Whiteman, R.; Lin, P.; Zhang, K.; Baumgart, H.; Abdel-Fattah, T.M. Controlled Synthesis of ZnO Nanorods Using Different Seed Layers. *ECS J. Solid State Sci. Technol.* **2020**, *9*, 121008. [[CrossRef](#)]
32. Kushch, S.D.; Kujunko, N.S.; Tarasov, B.P. Platinum nanoparticles on carbon nanomaterials with graphene structure as hydrogenation catalysts. *Russ. J. Gen. Chem.* **2009**, *79*, 706–710. [[CrossRef](#)]
33. Tang, Z.; Yin, X.; Zhang, Y.; Zhang, N.; Xu, Y. Inhibiting Pd nanoparticle aggregation and improving catalytic performance using one-dimensional CeO₂ nanotubes as support. *Chinese J. Catal.* **2013**, *34*, 1123–1127. [[CrossRef](#)]
34. Dushatinski, T.; Abdel-Fattah, T.M. Carbon Nanotube Composite Mesh Film with Tunable Optoelectronic Performance. *ECS J. Solid State Sci. Technol.* **2015**, *4*, M1–M5. [[CrossRef](#)]
35. Quach, Q.; Abdel-Fattah, T.M. Silver Nanoparticles functionalized Nanoporous Silica Nanoparticle grown over Graphene Oxide for enhancing Antibacterial effect. *J. Nanomater.* **2022**, *12*, 3341. [[CrossRef](#)] [[PubMed](#)]
36. Quach, Q.; Biehler, E.; Elzamzami, A.; Huff, C.; Long, J.M.; Abdel-Fattah, T.M. Catalytic Activity of Beta-Cyclodextrin-Gold Nanoparticles Network in Hydrogen Evolution Reaction. *Catalysts* **2021**, *11*, 118. [[CrossRef](#)]
37. Huff, C.; Long, J.M.; Abdel Fattah, T.M. Beta-Cyclodextrin-Assisted Synthesis of Silver Nanoparticle Network and Its Application in a Hydrogen Generation Reaction. *Catalysts* **2020**, *10*, 1014. [[CrossRef](#)]
38. Ma, X.; Liu, S.; Liu, Y.; Gu, G.; Xia, C. Comparative study on catalytic hydrodehalogenation of halogenated aromatic compounds over Pd/C and Raney Ni catalysts. *Sci. Rep.* **2016**, *6*, 25068. [[CrossRef](#)]
39. Gawande, M.B.; Goswami, A.; Felpin, F.X.; Asefa, T.; Huang, X.; Silva, R.; Zou, X.; Zboril, R.; Varma, R.S. Cu and Cu-Based Nanoparticles: Synthesis and Applications in Catalysis. *Chem. Rev.* **2016**, *116*, 3722–3811. [[CrossRef](#)]
40. Menshchikov, V.; Alekseenko, A.; Guterman, V.; Nechitailov, A.; Glebova, N.; Tomasov, A.; Spiridonova, O.; Belenov, S.; Zelenina, N.; Safronenko, O. Effective Platinum-Copper Catalysts for Methanol Oxidation and Oxygen Reduction in Proton-Exchange Membrane Fuel Cell. *J. Nanomater.* **2020**, *10*, 742. [[CrossRef](#)]
41. Motos, P.R.; Heijne, A.T.; Weijden, R.V.D.; Saakes, M.; Buisman, C.J.N.; Sleutels, T.H.J.A. High rate copper and energy recovery in microbial fuel cells. *Front Microbiol.* **2015**, *6*, 527.
42. Wu, N.; Ku, M.S. Enhanced TiO₂ photocatalysis by Cu in hydrogen production from aqueous methanol solution. *Int. J. Hydrogen Energy* **2004**, *29*, 1601–1605. [[CrossRef](#)]
43. Tang, Q.; Zhou, Z.; Chen, Z. Innovation and discovery of graphene-like materials via density-functional theory computations. *Wiley Interdiscip. Rev. Comput. Mol. Sci.* **2015**, *5*, 360–379. [[CrossRef](#)]
44. Das, V.K.; Shifrina, Z.B.; Bronstein, L.M. Graphene and graphene-like materials in biomass conversion: Paving the way to the future. *J. Mater. Chem. A* **2017**, *5*, 25131–25143. [[CrossRef](#)]
45. Samiee-Zafarghandi, R.; Hadi, A.; Karimi-Sabet, J. Graphene-supported metal nanoparticles as novel catalysts for syngas production using supercritical water gasification of microalgae. *Biomass Bioenergy* **2019**, *121*, 13–21. [[CrossRef](#)]
46. Zhou, Y.; Xie, C.; Su, L.; Han, X. Study of the risks of the graphene oxide preparation process by reaction calorimetry. *J. Therm. Anal. Calorim.* **2020**, *139*, 101–112. [[CrossRef](#)]
47. Adel, M.; El-Maghraby, A. Synthesis of few-layer graphene-like nanosheets from glucose: New facile approach for graphene-like nanosheets large-scale production. *J. Mater. Res.* **2016**, *31*, 455–467. [[CrossRef](#)]
48. Chen, Z.; Wang, W.; Zhang, Y.; Liang, Y.; Cui, Z.; Wang, X. Pd Nanoparticles Confined in the Porous Graphene-like Carbon Nanosheets for Olefin Hydrogenation. *Langmuir* **2018**, *34*, 12809–12814. [[CrossRef](#)]
49. Frindy, S.; Kadib, A.E.; Lahcini, M.; Primo, A.; García, H. Copper nanoparticles supported on graphene as an efficient catalyst for A₃ coupling of benzaldehydes. *Catal. Sci. Technol.* **2016**, *6*, 4306–4317. [[CrossRef](#)]
50. Kidambi, P.R.; Bayer, B.C.; Blume, R.; Wang, Z.J.; Baehtz, C.; Weatherup, R.S.; Willinger, M.G.; Schloegl, R.; Hofmann, S. Observing Graphene Grow: Catalyst–Graphene Interactions during Scalable Graphene Growth on Polycrystalline Copper. *Nano Lett.* **2013**, *13*, 4769–4778. [[CrossRef](#)]
51. Xiong, J.; Wang, Y.; Xue, Q.; Wu, X. Synthesis of highly stable dispersions of nanosized copper particles using L-ascorbic acid. *Green Chem.* **2011**, *13*, 900. [[CrossRef](#)]
52. Li, K.; Liu, Q.; Cheng, H.; Hu, M.; Zhang, S. Classification and Carbon Structural Transformation from Anthracite to Natural Coaly Graphite by XRD, Raman spectroscopy, and HRTEM. *Spectrochim. Acta Part A* **2021**, *249*, 119286. [[CrossRef](#)] [[PubMed](#)]
53. Mayoral, A.; Sakamoto, Y.; Anderson, P.A. Synthesis of Copper Chloride Nanowires by Thermal Treatment in the Presence of Zeolite X. *CrystEngComm* **2010**, *12*, 3012. [[CrossRef](#)]
54. Siddiqui, H.; Parra, M.R.; Qureshi, M.S.; Malik, M.M.; Haque, F.Z. Studies of structural, optical, and electrical properties associated with defects in sodium-doped copper oxide(CuO/Na) nanostructures. *J. Mater. Sci.* **2018**, *53*, 8826–8843. [[CrossRef](#)]
55. Khanna, P.K.; Gaikwad, S.; Adhyapak, P.V.; Singh, N.; Marimuthu, R. Synthesis and Characterization of Copper Nanoparticles. *Mater. Lett.* **2007**, *61*, 4711–4714. [[CrossRef](#)]
56. Antolini, E.; Cardellini, F. Formation of Carbon Supported PtRu Alloys: An XRD Analysis. *J. Alloys Compd.* **2001**, *315*, 118–122. [[CrossRef](#)]

57. Schlesinger, H.I.; Brown, H.C.; Finholt, A.E.; Gilbreath, J.R.; Hoekstra, H.R.; Hyde, E.K. Sodium Borohydride, Its Hydrolysis and its Use as a Reducing Agent and in the Generation of Hydrogen. *J. Am. Chem. Soc.* **1953**, *75*, 215–219. [[CrossRef](#)]
58. Kaufman, C.M.; Sen, B. Hydrogen Generation by Hydrolysis of Sodium Tetrahydroborate: Effects of Acids and Transition Metals and Their Salts. *J. Chem. Soc. Dalton Trans.* **1985**, *1985*, 307–313. [[CrossRef](#)]
59. Balbay, A.; Saka, C. Effect of phosphoric acid addition on the hydrogen production from hydrolysis of NaBH₄ with Cu based catalyst. *Energy Source Part A* **2018**, *40*, 794–804. [[CrossRef](#)]
60. Ding, X.-L.; Yuan, X.; Jia, C.; Ma, Z.-F. Hydrogen generation from catalytic hydrolysis of sodium borohydride solution using Cobalt–Copper–Boride (Co–Cu–B) catalysts. *Int. J. Hydrog. Energy* **2010**, *35*, 11077–11084. [[CrossRef](#)]
61. Huff, C.; Long, J.M.; Aboulatta, A.; Heyman, A.; Abdel-Fattah, T.M. Silver Nanoparticle/Multi-Walled Carbon Nanotube Composite as Catalyst for Hydrogen Production. *ECS J. Solid State Sci. Technol.* **2017**, *6*, M115–M118. [[CrossRef](#)]
62. Huff, C.; Long, J.M.; Heyman, A.; Abdel-Fattah, T.M. Palladium Nanoparticle Multiwalled Carbon Nanotube Composite as Catalyst for Hydrogen Production by the Hydrolysis of Sodium Borohydride. *ACS Appl. Energy Mater.* **2018**, *1*, 4635–4640. [[CrossRef](#)]
63. Huff, C.; Dushatinski, T.; Abdel-Fattah, T.M. Gold Nanoparticle/Multi-Walled Carbon Nanotube Composite as Novel Catalyst for Hydrogen Evolution Reactions. *Int. J. Hydrog. Energy* **2017**, *42*, 18985–18990. [[CrossRef](#)]
64. Biehler, E.; Quach, Q.; Huff, C.; Abdel-Fattah, T.M. Organo-Nanocups Assist the Formation of Ultra-Small Palladium Nanoparticle Catalysts for Hydrogen Evolution Reaction. *Materials* **2022**, *15*, 2692.
65. Huff, C.; Biehler, E.; Quach, Q.; Long, J.M.; Abdel-Fattah, T.M. Synthesis of highly dispersive platinum nanoparticles and their application in a hydrogen generation reaction. *Colloids Surf.* **2021**, *610*, 125734. [[CrossRef](#)]
66. Deraedt, C.; Salmon, L.; Gatard, S.; Ciganda, R.; Hernandez, E.; Ruiz, J.; Astruc, D. Sodium borohydride stabilizes very active gold nanoparticle catalysts. *Chem. Commun.* **2014**, *50*, 14194–14196. [[CrossRef](#)]
67. Wang, Z.; Li, G.; Hou, W.; Guo, H.; Wang, L.; Wu, M. Insights into the Use of Te–O Pairs as Active Centers of Carbon Nanosheets for Efficient Electrochemical Oxygen Reduction. *ACS Nano* **2023**, *17*, 8671. [[CrossRef](#)] [[PubMed](#)]
68. Zhang, B.; An, G.; Chen, J.; Guo, H.; Wang, L. Surface state engineering of carbon dot/carbon nanotube heterojunctions for boosting oxygen reduction performance. *J. Colloid Interface Sci.* **2023**, *637*, 173–181. [[CrossRef](#)] [[PubMed](#)]
69. Biehler, E.; Quach, Q.; Abdel-Fattah, T.M. Silver Nanoparticle-Decorated Fused Carbon Sphere Composite as a Catalyst for Hydrogen Generation. *Energies* **2023**, *16*, 5053. [[CrossRef](#)]

Disclaimer/Publisher’s Note: The statements, opinions and data contained in all publications are solely those of the individual author(s) and contributor(s) and not of MDPI and/or the editor(s). MDPI and/or the editor(s) disclaim responsibility for any injury to people or property resulting from any ideas, methods, instructions or products referred to in the content.